Published in final edited form as:
J Am Chem Soc. 2011 July 27; 133(29): 11389–11398. doi:10.1021/ja204524c.

Dramatic destabilization of transmembrane helix interactions by features of natural membrane environments

Heedeok Hong and **James U. Bowie***
Department of Chemistry and Biochemistry, UCLA-DOE Institute for Genomics and Proteomics, Molecular Biology Institute, University of California, Los Angeles, California 90095

Abstract

Membrane proteins have evolved to fold and function in a lipid bilayer, so it is generally assumed that their stability should be optimized in a natural membrane environment. Yet optimal stability is not always in accord with optimization of function, so evolutionary pressure, occurring in a complex membrane environment, may favor marginal stability. Here we find that the transmembrane helix dimer, glycophorin A (GpATM) is actually much less stable in the heterogeneous environment of a natural membrane than it is in model membranes and even common detergents. The primary destabilizing factors are electrostatic interactions between charged lipids and charged GpATM side chains, and non-specific competition from other membrane proteins. These effects overwhelm stabilizing contributions from lateral packing pressure and excluded volume. Our work illustrates how evolution can employ membrane composition to modulate protein stability.

Introduction

α-helical membrane proteins fold and assemble via lateral helix-helix interactions in bilayer membranes[1]. In addition to specific interactions within the protein, the membrane environment itself can play a major role in structuring membrane proteins[2]. Cell membranes are a highly heterogeneous medium in lipid and protein composition[3]. For example, *E. coli* inner membranes contain three major lipid species with different headgroups and the *E. coli* genome codes for more than a thousand putative α-helical membrane proteins[4,5]. Thus, there are a wide variety of potential interactions that could modulate transmembrane helix association through specific or nonspecific lipid-protein and protein-protein interactions. It is largely unknown how the complex lipid and protein environment of natural membranes influences the folding and stability of membrane proteins.

Bacterial and eukaryotic cell membranes are overall negatively charged and contain a significant fraction of nonbilayer lipids[6]. The negative charges of biological membranes help determine the topology of integral membrane proteins by electrostatic interactions with the charged residues[7–9]. The nonbilayer lipids such as phosphatidylethanolamine (PE) and lyso-phospholipid form inverted hexagonal (H_{II}) and hexagonal (H_I) phases, respectively, and thus strongly modulate the curvature stress and lateral pressure profile of the lipid bilayers[10]. These elastic properties can be important modulators of the structure, function, and topogenesis of many integral membrane proteins[2,11,12].

*Corresponding author: James U. Bowie, Boyer Hall, UCLA, 611 Charles E. Young Dr. E, Los Angeles, CA 90095-1570, bowie@mbi.ucla.edu.

Supporting Information Available. Supporting Figures 1–7. This material is available free of charge via the Internet at http://pubs.acs.org

In addition to the wide variety of lipids, membrane proteins occupy more than a half of total membrane mass[13]. The high concentration of proteins may perturb the structure and dynamics of the surrounding lipid molecules and reduce the surface area accessible for diffusion[14,15]. It is also possible that embedded membrane proteins can compete with specific protein-protein interactions in cell membranes.

Here, we investigated the effects of natural lipid and protein components on the stability of a specific transmembrane (TM) helix-helix interaction in reconstituted bilayer systems. TM helix interactions are prevalent in cell membranes and are involved in assembly, signaling, and subcellular localization of membrane proteins[16,17]. They have also served as an important model system for studying the lateral transmembrane helix–helix interactions that occur in the folding of α-helical membrane proteins[18,19]. As our model, we chose the well characterized glycophorin A transmembrane domain, GpATM, which forms a stable sequence-specific dimer in lipid environments. Extensive mutagenesis and thermodynamic studies have been carried out in detergent micelles and lipid bilayers to identify the driving forces determining the sequence specificity of the dimerization[20,21]. GpATM is sufficiently stable that it remains dimeric in SDS solution[20,22,23]. We recently found that GpATM is so stable in palmitoyloleoyl phosphatidylcholine ($C_{16:0}C_{18:1c9}$PC) model bilayers that it should be almost completely dimeric *in vivo*[24]. Nevertheless, the results of Duong *et al.* suggests that GpATM is mostly monomeric in *E. coli* inner membranes[25]. Chen *et al.* also reported that the wild-type GpATM is predominantly monomeric in bleb vesicles derived from mammalian cells[26]. These results suggest that there may be something different about natural membranes that destabilizes GpATM interactions relative to a pure $C_{16:0}C_{18:1c9}$PC bilayer.

Here we investigate the physico-chemical origin of this destabilization. Our results reveal several new aspects of lipid-protein and protein-protein interactions that can modulate the stability of transmembrane helix-helix interactions.

Results

The steric trap method

We used our recently developed steric trap method to measure the dimer stability of a staphylococcal nuclease-GpATM fusion, SNGpATM, in lipid bilayers[24,27]. The method, shown in Figure 1a and 1b has been described previously[24]. We attach two biotin tags that are sufficiently close in the dimer that only one biotin can be bound by a large monovalent streptavidin (mSA) molecule. Because of steric overlap, the second biotin tag can only be bound when the dimer falls apart to a monomer. Thus, the affinity of the second mSA binding is coupled to dissociation and therefore reflects dimer affinity. Binding is observed by monitoring the fluorescence of a pyrene label on SNGpATM. The method is applicable to high affinity interactions because dissociation can be thermodynamically driven by the high affinity of mSA and by its concentration. The affinity of mSA must be tuned to the affinity of the dimer interaction being examined. We therefore previously generated a series of monovalent streptavidin mutants whose biotin affinity range from ~10^{-9} M to ~10^{-6} M (Figure 1c)[24]. Employing a mSA variant with the appropriate affinity, biphasic binding is observed, corresponding to the high affinity binding of the first mSA, followed by SNGpATM dissociation and binding of the second mSA occurring at lower affinity. If the mSA affinity is too high, only one binding phase is observed because dimer affinity cannot compete with mSA binding.

Affinity of SNGpATM dimer is low in *E. coli* lipid membranes

To provide a lipid environment mimicking natural cell membranes, we measured the dissociation constant of a GpATM dimer in lipid bilayers composed of *E. coli* phospholipid extracts. *E. coli* inner membranes have a simpler lipid composition than eukaryotic cell membranes[4,28]. Due to the lack of cholesterol and sphingolipids, a complex lipid phase behavior in model membranes can be avoided[29,30]. More importantly, dimerization of GpATM has been extensively studied in *E. coli* inner membranes *in vivo* using the TOXCAT assay so that our results can be directly compared with the previous reports[25,31].

SNGpATM in *E. coli* lipid membranes was titrated with a series of mSA mutants with different intrinsic biotin binding affinities ($K_{d,biotin}$) (Figure 2b). Only a single tight binding phase was observed with the stronger biotin binding mSA mutants mSA-S45A ($K_{d,biotin}$=2.1×10^{-9} M), mSA-E44Q/S45A ($K_{d,biotin}$=9.1×10^{-9} M), and mSA-W79M ($K_{d,biotin}$=4.5×10^{-8} M), indicating that the affinity of these mSA variants was too high to effectively measure the SNGpATM dissociation constant. The characteristic two phase binding curve could be obtained with a weaker biotin binding mSA-N23A/S45A ($K_{d,biotin}$=8.6×10^{-7} M) (for the detailed procedure, see Supporting Figure 2). The fitted dissociation constant ($K_{d,GpA}$) of the GpATM dimer was 1.0±0.3×10^{-8} M. By comparison, the dissociation constant in pure $C_{16:0}C_{18:1c9}$PC bilayers was 1.5±0.6×10^{-12} M and required the use of higher affinity mSA variant, mSA-E44Q/S45A ($K_{d,biotin}$=9.1×10^{-9} M) (Figure 2a). Thus, the affinity of GpATM dimer was severely weakened in *E. coli* lipid membranes relative to $C_{16:0}C_{18:1c9}$PC membranes by $\Delta\Delta G^{o}_{x,Dissociation}$ =~5 kcal/mol using a mol-fraction scale[32]. Surprisingly, the affinity is not much different than in detergent micelle solutions (Figure 2c)[32,33].

Host-guest system to test the effects of individual lipid components

To dissect the bilayer forces that contribute to the destabilization of the GpATM dimer in *E. coli* lipid membranes, we set out to test the effects of the major lipid components of *E. coli* inner membranes which are composed of 70~75 % of zwitterionic phophatidylethanolamine (PE), 15~20% of negatively charged phosphatidylglycerol (PG), and 5~10 % of negatively charged cardiolipin (CL) lipids. The major hydrocarbon composition is 30~45 % of 16:0, 30~45 % of 16:1*c9*, and 15~30 % of 18:1c_{11}[4].

We designed a host-guest lipid system, which is composed of purely synthetic phospholipids. $C_{16:0}C_{18:1c9}$PC was chosen as a host lipid, and the guest lipids, which have a various headgroup structure but the same hydrocarbon composition ($C_{16:0}C_{18:1c9}$), were incorporated into the lipid bilayers to an appropriate ratio. The hydrocarbon composition was fixed to $C_{16:0}C_{18:1c9}$ because *E. coli* lipids have a similar phase behavior to palmitoyloleoyl phosphatidylethanolamine ($C_{16:0}C_{18:1c9}$PE)[4]. We chose naturally abundant $C_{16:0}C_{18:1c9}$PE, $C_{16:0}C_{18:1c9}$PG, lyso-phosphatidylcholine ($C_{18:1c9}$PC), palmitoyloleoyl phosphatidylserine ($C_{16:0}C_{18:1c9}$PS), and cardiolipin (*tetra*-$C_{18:1c9}$CL) as guest lipids. Thus, in the lipid bilayers with different lipid compositions, the variations in the hydrophobic thickness were minimized so that the dominant headgroup effects could be studied.

Bilayer lateral pressure modulates transmembrane helix-heix interaction

First, we tested the effect of PE lipids on the dimerization of GpATM. PE lipids with longer acyl chains and *cis*-double bonds form an inverted hexagonal phase (H_{II}) above the liquid-hexagonal phase transition temperature [34]. When incorporated into a bilayer, they induce an intrinsic negative curvature in each monolayer leaflet and increase the lateral pressure in the central region of the bilayer[35,36]. Although highly stable in pure $C_{16:0}C_{18:1c9}$PC bilayers ($K_{d,GpA}$=1.5±0.6 ×10^{-12} M at lipid-to-protein molar ratio (*L/P*)=1000, Figure 2a), the GpATM dimer became even more stable in $C_{16:0}C_{18:1c9}$PE/PC (40/60 in mol-%) bilayers

($K_{d,GpA}$=2.1±0.5 ×10^{-13} M at *L/P*=1100). At a comparable *L/P* ratio, the net stabilization effect by 40 % $C_{16:0}C_{18:1c9}$PE was $\Delta\Delta G^{o}_{x,Dissociation}$ =−1.5 kcal/mol relative to pure $C_{16:0}C_{18:1c9}$PC bilayers.

A complication with the incorporation of the small headgroup PE lipid into PC bilayers is that it increases not only the lateral pressure but also the hydrophobic thickness of the bilayers[37]. Thus, dimer stability was tested in 100 % $C_{18:0}C_{18:1c9}$PC bilayers (Supporting Figure3). $C_{18:0}C_{18:1c9}$PC has a thicker hydrocarbon thickness (d_{hc}=27.6 Å[37]) than $C_{16:0}C_{18:1c9}$PC (d_{hc}=26.5 Å[38]) and has a similar gel-to-liquid phase transition temperature (T_m=13 °C[39]) as $C_{16:0}C_{18:1c9}$PC/PE (60/40) mixed bilayers (T_m=~12 °C[40]). The T_m and d_{hc} of pure $C_{16:0}C_{18:1c9}$PE are 24 °C[40] and 30.1 Å[37], respectively. Increasing the hydrocarbon thickness from $C_{16:0}C_{18:1c9}$PC to $C_{18:0}C_{18:1c9}$PC destabilized the GpATM dimer. Thus, the net stabilization effect by PE lipid likely originates from the increase in the bilayer lateral pressure rather than the increase in thickness.

To further test the lateral pressure effect on the stability of the GpATM dimer, the micelle-forming lyso-phosphatidylcholine ($C_{18:1c9}$PC) was perfused into the $C_{16:0}C_{18:1c9}$PC-SNGpATM proteoliposomes to a final 20 mol-% of the total lipids. In constrast to PE lipids, lysoPC induces a positive intrinsic monolayer curvature and reduces the lateral pressure in the bilayer center[2]. In the bilayers containing $C_{18:1c9}$PC, the dimer stability was dramatically reduced by ~4.5 kcal/mol (Figure 3b and 3c) relative to pure $C_{16:0}C_{18:1c9}$PC bilayers. These results again suggest that packing pressure has a significant effect on dimer stability. The presence of PE in *E. coli* membranes, which increases lateral packing pressure, is therefore not likely to be the origin of the destabilization of the SNGpATM dimer.

Strong destabilization of TM helix interactions in negatively charged membranes

The effects of the negatively charged lipids PG and PS on the dimerization of GpATM were tested in $C_{16:0}C_{18:1c9}$PG/PC (20/80) and $C_{16:0}C_{18:1c9}$PS/PC (20/80) bilayers. PG is the major negatively charged lipid in *E. coli* inner membranes while PS is the major negatively charged lipid in eukaryotic cell membranes. As shown in Figure 4, the stability of the GpATM dimer dramatically decreased in the negatively charged membranes by $\Delta\Delta G^{o}_{x,Dissociation}$= 4.5~5 kcal/mol relative to pure $C_{16:0}C_{18:1c9}$PC bilayers (Figure 4a, and 4b filled circles, also see Supporting Figure 4). Moreover, the chemical structure of the lipid headgroup is not a factor since the incorporation of either PG and PS lipids decreased the stability of the GpATM dimer to a similar level as *E. coli* lipids (Figure 4d). Incorporation of 5 mol-% of cardiolipin (*tetra*-$C_{18:1c9}$CL) also destabilized the dimer, but only to a moderate extent (Supporting Figure 5).

It is possible that the negatively charged membranes increased streptavidin binding affinity, thereby falsely reporting a weakened GpATM dimerization affinity. We therefore tested the intrinsic binding affinity of mSA to a monomeric GpATM mutant, GpATM-G83I mutant, so that dimerization and mSA binding affinity could be separated. In $C_{16:0}C_{18:1c9}$PC/PG (20/80) bilayers (Figure 4a, filled triangles), the overall binding curve closely overlapped the intrinsic biotin binding curve of mSA-N23A/S45A, as expected for binding to a monomeric variant. In addition, dilution of SNGpATM by a higher concentration of $C_{16:0}C_{18:1c9}$PG/PC lipids also shifted the second phase binding curve to lower mSA concentration region, consistent with destabilization of the dimer (Figure 4c). Therefore, we could conclude that the specificity of dimer formation is maintained in the negatively charged membranes. The intrinsic biotin binding affinity of mSA mutants did not change in the negatively charged membranes except for mSA-S27R, whose intrinsic affinity increased by only 2.3 times in the $C_{16:0}C_{18:1c9}$PG/PC bilayers (Supporting Figure 1).

We next tested if the stability enhancing effect by the nonbilayer PE lipid and the stability reducing effect by the negatively charged PG or PS are additive when these two lipid species were incorporated at the same time in lipid bilayers. The resulting lipid compositions ($C_{16:0}C_{18:1c9}$PE/PG/PC or PS) are more similar to those of *E. coli* inner membrane or eukaryotic cell membranes. As before (see above), the addition of 40 mol-% $C_{16:0}C_{18:1c9}$PE to 20 mol-% PG or 20 mol-% PS mildly increased the dimer stability by $\Delta\Delta G^o_{x,Dissociation}$= −0.5±0.4 kcal/mol in PS-containing membranes and $\Delta\Delta G^o_{x,Dissociation}$=−0.6±0.3~−0.9±0.4 kcal/mol in PG-containing membranes, respectively (Figure 4a and 4b, open circles). The stability enhancement, however, was smaller than in neutral $C_{16:0}C_{18:1c9}$PE/PC (40/60) bilayers, however ($\Delta\Delta G^o_{x,Dissociation}$=−1.5 kcal/mol, Figure 3c).

Electrostatic interaction between negatively charged lipids and the positive charge residues of TM helix is responsible for the destabilization

What is the origin of the strong destabilization of GpATM dimer induced by the negatively charged lipids? GpATM contains four positively charged residues, Arg96, Arg97, Lys100, and Lys101 (ITLIIFGVMAGVIGTILLISYGI**RR**LI**KK**LG: TM domain underlined, and Arg and Lys residues in bold.) in the C-terminal region of the transmembrane domain[23]. In an erythrocyte membrane, these residues are likely to be located in the membrane-cytoplasm interfacial region. We therefore hypothesized that electrostatic interactions between the interfacial positively charged residues and the negatively charged lipid headgroups may affect the dimerization equilibrium of GpATM.

To address this question, a quadruple mutant R96Q/R97Q/K100N/K101N ($GpATM_{RRKK/QQNN}$) was generated, in which all the C-terminal positively charged residues were replaced by neutral polar residues. This construct showed the similar dimer stability to wild-type SNGpATM in non-denaturing decyl malotoside (DM) micelles (Figure 5a). When the stability of the $GpATM_{RRKK/QQNN}$ dimer was measured in the negatively charged $C_{16:0}C_{18:1c9}$PG/PC (20/80) and the neutral $C_{16:0}C_{18:1c9}$PC bilayer, the destabilization effect of the negatively charged lipids was completely eliminated (Figure 5b and 5c). The dissociation constants of the $GpATM_{RRKK/QQNN}$ dimer in the neutral and negatively charged bilayers ($K_{d,GpA}$ =5.8±2.4×10^{-13} M in $C_{16:0}C_{18:1c9}$PC and $K_{d,GpA}$ =7.3±4.1×10−^{13} M in $C_{16:0}C_{18:1c9}$PG/PC) were indistinguishable and close to the dissociation constant of wild-type GpATM dimer in neutral $C_{16:0}C_{18:1c9}$PC bilayers ($K_{d,GpA}$ =1.5±0.6×10^{-12} M). This result strongly suggests that the specific electrostatic interaction between the interfacial positively charged residues of GpATM and the negatively charged membranes strongly reduce the stability of the GpATM dimer.

Incorporation of *E. coli* inner membrane proteins leads to a significant destabilization of specific TM helix-helix interactions in membranes

To investigate the effects of heterogeneous membrane proteins on the specific dimerization of TM helices, the total inner membrane proteins (IMP) of *E. coli* cells were solubilized, and reconstituted in *E. coli* lipid membranes with SNGpATM (Supporting Figure 6a and 6c). As shown in Figure 6a, the incorporation of IMPs dramatically decreased the SNGpATM dimer affinity. The overall mSA-binding curve reached an intrinsic biotin binding regime of mSA-S27R ($K_{d,biotin}$ =2.8×10^{-6} M) at the IMP-SNGpATM mass ratio of 0.22. Therefore, in *E. coli* lipid membranes, the presence of a relatively small amount of general *E. coli* inner membrane proteins led to a large destabilization of the GpATM dimer to the level where the dissociation constant ($K_{d,GpA}$) of the dimer was so weak that it could not be measured by the steric trapping. The mass ratio of the total reconstituted membrane proteins (SNGpATM plus IMPs) to phospholipids was approximately 1:7.0 at the highest IMP content in the proteoliposomes, which is considerably more dilute than the total protein-to-lipid mass ratio of 2.8:1 of the solubilized *E. coli* inner membranes.

To quantitatively assess the destabilization effect by IMPs at higher IMP-SNGpATM mass ratio, SNGpATM and IMPs were reconstituted in pure $C_{16:0}C_{18:1c9}$PC bilayers, in which the GpATM dimer is highly stable (Figure 6b and Supporting Figure 6d). The high stability in $C_{16:0}C_{18:1c9}$PC bilayers allows a wider range of the destabilizing effects to be quantitatively assessed than is possible in *E. coli* lipid membranes. As the protein to lipid mass ratio increased from 0 to 1.0, the dissociation constants increased from $K_{d,GpA}$ =3.0×10^{-12} M to $K_{d,GpA}$ =9.2±2.9×10^{-9} M or ~3 orders of magnitude at *L/P*=1400~1600 (Supporting Figure 7). At the highest IMP-SNGpATM mass ratio tested, the net destabilization free energy of the dimer amounted to remarkable $\Delta\Delta G^{o}_{x,Dissociation}$=4~5 kcal/mol.

DISCUSSION

Here we showed that individual lipid components differentially affect the dimerization equilibrium of GpATM and that generic membrane proteins extracted from the *E. coli* inner membranes significantly destabilized the TM helix-helix interaction in lipid bilayers. The combination of these environmental factors imposes strong destabilizing forces on the GpATM dimer. Our results are summarized in Figure 7a. In pure $C_{16:0}C_{18:1c9}$PC bilayers, the dimer stability is ΔG_x ~12 kcal/mol. The addition of the negatively charged lipid $C_{16:0}C_{18:1c9}$PG in the proportion seen in *E. coli* membranes destabilizes the dimer about ~5 kcal/mol due to electrostatic interactions between the membrane and the protein. The *E. coli* lipid $C_{16:0}C_{18:1c9}$PE increases stability by about ~−1 kcal/mol through an increase in lateral packing pressure. Finally, the addition of *E. coli* IMP, which recreates a facsimile of a natural *E. coli* membrane environment, destabilized the dimeric form by roughly ~5 kcal/mol to a level of ΔG_x ~ 3 kcal/mol. This value is remarkably similar to the values estimated in membrane blebs by Chen *et al.* [26]. Our results provide a clearer picture of the physico-chemical origin of the relatively weak GpATM dimerization seen in these natural membranes.

Membrane proteins occupy a significant fraction of the total membrane surface, reducing the area accessible to the free diffusion of the embedded proteins[15]. Grasberger *et al.* suggests that the excluded volume effect of inert proteins should increase the dimerization equilibrium constant by about 2.7 kcal/mol when the fractional occupancy of the inert proteins increases up to 0.5 [41]. We find the opposite effect, however. At a mass ratio of ~1, the GpATM dimer is destabilized by 4~5 kcal/mol. It seems likely that this effect is due to competition for the binding surface with other potential protein partners in the crowded membrane. Certainly, the GxxxG dimerization motif of GpATM is not uncommon in other membrane proteins[42]. We cannot exclude the possibility that the added membrane proteins may alter lipid structure, however[14]. Although the relative concentration of IMP in our experimental condition is less than in real *E. coli* cell membranes, the destabilization effect already exceeds the expected stabilization effect of excluded volume, indicating the importance of nonspecific interactions in determining the stability of helix-helix interactions cell membranes. The potential for non-specific contributions could be a significant complication when evaluating the effects of mutations using *in vivo* systems or predicting *in vivo* effects from *in vitro* studies.

We have made the first direct thermodynamic measurements on the role of the bilayer lateral pressures in the TM helix-helix associations of α-helical membrane proteins (Figure 3). Increasing the lateral pressure by 40 % inverted hexagonal phase forming PE increased the dimer stability by $\Delta\Delta G_x$ = ~−1.5 kcal/mol while decreasing lateral pressure with 20 % micellar lysoPC exerted the opposite effect ($\Delta\Delta G_x$=~4.5kcal/mol destabilization). Many studies have demonstrated the profound effects of bilayer elastic properties on the structure, function, and folding of integral membrane proteins[2]. For example, the open states of several mechanosensitive channels are stabilized by addition of lysoPCs[43–45]. Electron

paramagnetic resonance (EPR) studies showed that the incorporation of lysoPC induces a dramatic structural rearrangement of MscL[44] and MscS[45]. The effects of the lateral pressure induced by PE lipids are manifested in opposite ways for two channel forming antimicrobial peptides, alamethicin[46] and gramicidin[47]. The incorporation of PE lipids increases the conductance level and open lifetime of alamethicin, a transmembrane peptide, by facilitating the lateral association of the peptides. In contrast, PE lipids decrease the channel activity of gramicidin, which spans half of a full bilayer thickness. The modification of lateral pressure profile also significantly changes the refolding yield and kinetics of α-helical membrane proteins[48,49] and the thermodynamic stability of β-barrel membrane proteins[50]. It is still not clear how and why the lateral pressure affects the conformation of membrane proteins. In general, the higher lateral pressure condition seems to favor the association and packing of the transmembrane secondary structure elements. Exposure of the protein surfaces of the associated and folded state of the membrane proteins may be more energetically costly under high lateral pressure. In addition, the hourglass shapes of most integral membrane proteins of known structures may relieve the negative monolayer curvature strains induced by PE lipids stabilizing the folded state[50,51]. In the case of GpATM, the helices splay from the central GxxxG packing interface[52,53], so that the volume of the dimer should be higher at the edges of the bilayer—a structure that would be favored by the positive pressure in the center and negative pressure at the edges.

We were able to reproduce degree of destabilization by *E. coli* lipids in entirely synthetic lipid membranes by introducing negatively charged lipids. The electrostatic interactions between the negatively charged lipid headgroups and the positively charged residues in the cytosolic side of the GpATM played a prominent role in this phenomenon. As illustrated in Figure 7b, the interfacial charge interactions could either alter the structure of the dimer or the monomer, thereby reducing the net stability of the dimeric form. All biological membranes are essentially negatively charged and the positively charged residues of membrane proteins are significantly enriched near the bilayer-water interface in the cytoplasmic side of the membranes[54]. This biased charge distribution, called ‘the positive-inside rule’ serves as a strong determinant of membrane protein topology. Although the polar lipid headgoups mostly comprise the interfacial region, this region is not fully hydrated[55]. Therefore, electrostatic interactions can be much stronger than in the bulk water phase. It has been frequently observed that the hydrocarbon region of Lys or Arg side chains in membrane proteins are buried in the bilayer core and the polar charged group is anchored in the water-bilayer interface[56]. This snorkeling effect may help the stabilization and precise positioning of α-helical segments of membrane proteins in lipid bilayers[57]. Our results strongly suggest that the electrostatic interactions between the interfacial Lys and Arg residues and the negatively charged membranes [58], not only determine the topology but also may strongly affect the energetics of the TM helix-helix associations in membrane proteins or their complexes.

The relatively non-specific environmental factors examined in this work highlight a tool evolution can employ to adjust membrane protein interactions to a level appropriate for function. Indeed, evolutionary pressure does not generally favor optimal stability. Random mutations tend to drive proteins toward marginal stability and functional constraints can also demand low stability[59]. Protein stabilization involves a complex balance of forces involving interactions within the protein itself and between the protein and the environment[1]. Our work illustrates how evolution can employ the relatively structured membrane environment to modulate stability in accord with evolutionary pressure.

MATERIALS and METHODS

Cloning, expression and purification of SNGpATM with biotin acceptor peptide tag

The pET11a vector encoding staphylococcal nuclease-glycorphorinA transmembrane domain fusion (SNGpATM) was a gift from Karen Fleming (Johns Hopkins University). The detailed procedures for the cloning, expression, and purification of SNGpATM with biotin acceptor peptide (BAP) tag were described previously [60]. The gene encoding $SNGpATM_{RRKK/QQNN}$ was generated by mutating Lys100 and Lys101 to Asn100 and Asn101 at the same time using the primer 5'-GGT ATT TCC TCA CTG ATA AAT AAC CTC GAG CAC CAC CAC followed by simultaneously substituting Arg96 and Arg97 for Gln96 and Gln97 with the primer 5'-TTA ATT TCT TAC GGT ATT CAA CAA CTG ATA AAT AAC CTC G.

Preparation of total *E. coli* inner membrane proteins

E. coli (BL21(DE3)Rp strain, Agilent Techonologies) cells were grown at 37 °C in LB media containing 0.5 mM chloramphenicol to an OD600nm ~ 0.9. The harvested cells were resuspended in 20 ml of 50 mM TrisHCl buffer (pH 8.0) containing 20 % glycerol and lyzed using a French press four times at 8,000 psi. The resuspension was diluted with an equal volume of the resuspension buffer and centrifuged at 4,000 g for 10 minutes. The supernatant was then centrifuged at 40,000 g for 90 minutes in an ultracentrifuge (Optima L-90K, Beckman-Coulter) to obtain the total membrane fraction. The pellet was resuspended and washed with 10 ml of 50 mM TrisHCl buffer (pH 8.0) containing 20 % sucrose and 4 M urea. The resuspension was loaded to the top of a continuous sucrose gradient (30~60 % sucrose) prepared in a Quick-Seal centrifuge tube (38×102 mm, Beckman Instruments) and centrifuged at 27,000 rpm in a 45 K rotor for 16 hours. The red-colored inner membrane fraction layer was collected in a 25 ml volume using a syringe with 18G needle. The collected inner membranes were diluted 5 times with 50 mM TrisHCl (pH 8.0) without sucrose and centrifuged again at 27,000 rpm for 1 hour in the 45 Ti rotor. The pellet was solubilized with 3 ml of 4 % decylmaloside (DM) solution (pH 8.0 50 mM TrisHCl, 200 mM NaCl) and centrifuged at 13,000 rpm for 5 minutes. The total concentrations of phospholipids and proteins in the supernatant were determined by an organic phosphate assay[61] and a BioRad Dc assay, respectively. The final stock solution contained 4.2 mM of phospholipids and 8.5 mg/ml of proteins.

Preparation of proteoliposomes

E. coli polar extract lipids and synthetic phospholipids were purchased from Avanti polar lipids in chloroform solutions. Typically, 10 μmol of pure lipids or lipid mixtures dissolved in chloroform were added to glass tubes and dried under a stream of nitrogen gas. The residual solvent was further removed in a vacuum dessiccator for 2 hours. The dried lipid films were hydrated and solubilized in 1 ml of 3 % β-octylglucoside (Anatrace, Anagrade), 20 mM MOPS, 200 mM NaCl (pH 7.5). The SNGpATM stock solution (290~350 μM) in DM was added to the solubilized lipids at a final concentration of 10 μM and incubated at room temperature for 1 hour. SNGpATM was reconstituted into lipid vesicles by dialyzing against 250 sample volumes of 20 mM MOPS, 200 mM NaCl buffer solution (pH 7.5), with three buffer exchanges over 48 hours at 5 °C (Spectra/Por 25 kDa cut-off dialysis membrane, 7.5 mm diameter). The resulting proteoliposomes were passed through Nucleo track etch membrane (Whatman) with 200 nm pore-sizes using a mini-extruder (Avanti polar lipids) 15 times. To prepare the lipid vesicles containing 20 mol-% lysoPC ($C_{18:1c9}PC$), the dialyzed pure $C_{16:0}C_{18:1c9}PC$ proteoliposomes containing SNGpATM was mixed with the micellar solution of $C_{18:1c9}PC$, incubated at room temperature for 5 hours, and extruded with the 200 nm pore size membrane. The typical average diameter of

proteoliposomes was 110 ±60 nm as measured by dynamic light scattering (DynaPro light-scattering systems, Protein Solutions). The liposomal solutions were stored at 4 °C.

Determination of protein and lipid concentrations in proteoliposomes

The proteolipsomes prepared above were solubilized with an equal volume of 200 mM C_8E_5 solution (20 mM MOPS, 200 mM NaCl, pH 7.5). To determine SNGpATM concentration, the solubilized sample was titrated with wild-type mSA and incubated overnight. The total concentration of biotinylated pyrene-labeled SNGpATM was determined by fitting the stoichiometric binding data with a fixed parameter, $K_{d,biotin}=10^{-14}$ M. The total lipid concentration in proteoliposome samples was measured by an organic phosphate assay[61]. The orientation distributions of reconstituted GpATM in proteoliposomes were determined by avidin binding assay as described previously[24].

Monovalent streptavidin binding measurements in detergent micelles and bilayers

For binding measurements in detergent micelles, 2 μM of biotinylated pyrene-labeled wild-type or mutant SNGpATMs were titrated with monovalent streptavidin (mSA) in buffer solutions containing 40 mM DM (Anatrace, Anagrade), 20 mM 3-(N-morpholino)propanesulfonic acid (MOPS), and 200 mM NaCl (pH 7.5). A total volume of 70 μl of each sample was transferred to a 96-well UV-compatible microplate (BD-Falcon), sealed with a polyolefin tape, and incubated overnight at room temperature. Binding of mSA coupled with the dissociation of the SNGpATM dimer was monitored by pyrene monomer fluorescence at 390 nm with an excitation wavelength of 330 nm using a SpectraMax M5 plate reader (Molecular Devices). At the end of the measurements, excess free biotin was added to a final concentration of 2 mM and incubated more than 1 hour at room temperature to dissociate bound mSA from the biotinylated SNGpATM. The pyrene fluorescence intensity was measured at least five times for the biotin added samples and used as the background. The background-subtracted data were fitted to Eq. (1) to extract the dissociation constants ($K_{d,GpA}$) of the SNGpATM dimer.

For binding measurements in lipid vesicle solution, 20~40 μl of proteliposomes was mixed with various compositions of buffer/BSA (bovine serum albumin, Sigma)/mSA mixtures. BSA was added to match the total protein concentrations of the sample solutions which can affect osmolarity. The total molar concentration of BSA and mSA was adjusted to 100 μM in all sample solutions. A total volume of 80 μl of each sample was transferred to a microplate, sealed with a polyolefin tape. When the lipid vesicles were composed of neutral zwitterionic lipids such as PC and PE, the samples were incubated overnight. When the vesicles contained negatively charged lipids such as *E. coli* polar extract, PG, or PS, the samples were incubated for 2~3 hours. The same instrumental parameters as in the micellar solutions were used. The mSA-induced changes in the pyrene-fluorescence intensity were measured at least 5 times and averaged. At the end of the measurements, excess free biotin was added to a final concentration of 2 mM and incubated more than 6 hours for the samples containing strong biotin binding mSA mutants (mSA-S45A, -E44Q/S45A, -W79M, and -W79L) and for 1 hour for the samples containing weak biotin binding mSA mutants (mSA-N23A/S45A and –S27R) at room temperature to dissociate bound mSA from the biotinylated SNGpATM. The fluorescence data from the biotin-blocked samples, which were averaged from at least 5 times of measurements at least, served as a background. The background-subtracted data were fitted to the Eq. (1) or Eq. (2) to extract $K_{d,GpA}$ of the SNGpATM dimer[24].

$$F_\theta = A_1 \frac{-(1+\frac{K_{d,biotin}}{[mSA]}) + ((1+\frac{K_{d,biotin}}{[mSA]})^2 + 8P_0 \frac{K_{d,biotin}^2}{K_{d,biotin}} \frac{1}{[mSA]^2})^{1/2}}{4P_0 \frac{K_{d,biotin}^2}{K_{d,GpA}} \frac{1}{[mSA]^2}} + A_2 \quad (1)$$

$$F_\theta = A_1 \frac{(P_0 + [mSA] + K_{d,biotin}) - [(P_0 + [mSA] + K_{d,biotin})^2 - 4P_0[mSA]]^{1/2}}{2P_0} + A_2 \frac{-(1+\frac{K_{d,biotin}}{[mSA]}) + ((1+\frac{K_{d,biotin}}{[mSA]})^2 + 8P_0 \frac{K_{d,biotin}^2}{K_{d,biotin}} \frac{1}{[mSA]^2})^{1/2}}{4P_0 \frac{K_{d,biotin}^2}{K_{d,GpA}} \frac{1}{[mSA]^2}} + A_3 \quad (2)$$

, where F_θ is the change in the specific binding signal of mSA, P_o is the mSA-accessible SNGpATM concentration, A_1 and A_2 are the amplitudes of the binding phase and initial fluorescence level, respectively, [mSA] is the total mSA concentration, and $K_{d,biotin}$ is the intrinsic biotin dissociation constant for mSA. When an ideal two phase binding curve was obtained with a strong biotin binding mSA mutant (mSA-S45A, -E44Q/S45A, -W79M, and -W79L), a simultaneous fitting of the first and the second binding phase (Eq. (1)) was applied. But when a weaker mSA mutant was used (mSA-N23A/S45A and -S27R), the second binding phase was selectively fitted to Eq. (2). The onset of the second binding phase was identified by the breaking point of the first derivative of the overall binding curve[24].

Supplementary Material

Refer to Web version on PubMed Central for supplementary material.

Acknowledgments

This work was supported by NIH Grants R01GM063919 and R01GM081783 to J.U.B.. H.H. is supported by the Leukemia and Lymphoma Society Career Development Award (Fellow). We thank Karen Fleming lab (Johns Hopkins University) and Alice Ting lab (MIT) for providing plasmids, and Bowie lab members for critically reading the manuscript.

REFERENCES

1. Bowie JU. Nature. 2005; 438:581–589. [PubMed: 16319877]
2. Andersen OS, Koeppe RE 2nd. Annu Rev Biophys Biomol Struct. 2007; 36:107–130. [PubMed: 17263662]
3. Sachs JN, Engelman DM. Annu Rev Biochem. 2006; 75:707–712. [PubMed: 16756508]
4. Morein S, Andersson A, Rilfors L, Lindblom G. J Biol Chem. 1996; 271:6801–6809. [PubMed: 8636103]
5. Wallin E, von Heijne G. Protein Sci. 1998; 7:1029–1038. [PubMed: 9568909]
6. de Kruijff B. Curr Opin Chem Biol. 1997; 1:564–569. [PubMed: 9667894]
7. van Klompenburg W, de Kruijff B. J Membr Biol. 1998; 162:1–7. [PubMed: 9516232]
8. von Heijne G. Nat Rev Mol Cell Biol. 2006; 7:909–918. [PubMed: 17139331]
9. Bogdanov M, Xie J, Dowhan W. J Biol Chem. 2009; 284:9637–9641. [PubMed: 19074771]
10. Seddon JM. Biochim Biophys Acta. 1990; 1031:1–69. [PubMed: 2407291]
11. Rietveld AG, Koorengevel MC, de Kruijff B. Embo J. 1995; 14:5506–5513. [PubMed: 8521807]
12. Dowhan W, Bogdanov M. Annu Rev Biochem. 2009; 78:515–540. [PubMed: 19489728]
13. Raetz CR. Microbiol Rev. 1978; 42:614–659. [PubMed: 362151]

14. Mitra K, Ubarretxena-Belandia I, Taguchi T, Warren G, Engelman DM. Proc Natl Acad Sci U S A. 2004; 101:4083–4088. [PubMed: 15016920]
15. Engelman DM. Nature. 2005; 438:578–580. [PubMed: 16319876]
16. Matthews EE, Zoonens M, Engelman DM. Cell. 2006; 127:447–450. [PubMed: 17081964]
17. Moore DT, Berger BW, DeGrado WF. Structure. 2008; 16:991–1001. [PubMed: 18611372]
18. Fleming KG, Engelman DM. Proc Natl Acad Sci U S A. 2001; 98:14340–14344. [PubMed: 11724930]
19. Rath A, Tulumello DV, Deber CM. Biochemistry. 2009; 48:3036–3045. [PubMed: 19278229]
20. Lemmon MA, Flanagan JM, Treutlein HR, Zhang J, Engelman DM. Biochemistry. 1992; 31:12719–12725. [PubMed: 1463743]
21. Doura AK, Fleming KG. J Mol Biol. 2004; 343:1487–1497. [PubMed: 15491626]
22. Bormann BJ, Knowles WJ, Marchesi VT. J Biol Chem. 1989; 264:4033–4037. [PubMed: 2783929]
23. Lemmon MA, Flanagan JM, Hunt JF, Adair BD, Bormann BJ, Dempsey CE, Engelman DM. J Biol Chem. 1992; 267:7683–7689. [PubMed: 1560003]
24. Hong H, Blois TM, Cao Z, Bowie JU. Proc Natl Acad Sci U S A. 2010; 107:19802–19807. [PubMed: 21041662]
25. Duong MT, Jaszewski TM, Fleming KG, MacKenzie KR. J Mol Biol. 2007; 371:422–434. [PubMed: 17570394]
26. Chen L, Novicky L, Merzlyakov M, Hristov T, Hristova K. J Am Chem Soc. 2010; 132:3628–3635. [PubMed: 20158179]
27. Blois TM, Hong H, Kim TH, Bowie JU. J Am Chem Soc. 2009; 131:13914–13915. [PubMed: 19739627]
28. van Meer G, Voelker DR, Feigenson GW. Nat Rev Mol Cell Biol. 2008; 9:112–124. [PubMed: 18216768]
29. Rand RP, Fuller N, Parsegian VA, Rau DC. Biochemistry. 1988; 27:7711–7722. [PubMed: 3207702]
30. Crane JM, Tamm LK. Biophys J. 2004; 86:2965–2979. [PubMed: 15111412]
31. Russ WP, Engelman DM. Proc Natl Acad Sci U S A. 1999; 96:863–868. [PubMed: 9927659]
32. Fleming K. G. J Mol Biol. 2002; 323:563–571.
33. Fisher LE, Engelman DM, Sturgis JN. Biophys J. 2003; 85:3097–3105. [PubMed: 14581210]
34. Tate MW, Gruner SM. Biochemistry. 1987; 26:231–236. [PubMed: 3828299]
35. Cantor RS. Biophys J. 1999; 76:2625–2639. [PubMed: 10233077]
36. Gruner SM. Proc Natl Acad Sci U S A. 1985; 82:3665–3669. [PubMed: 3858841]
37. Rand RP, Parsegian VA. Biochim Biophys Acta. 1989; 988:351–376.
38. Lewis BA, Engelman DM. J Mol Biol. 1983; 166:211–217. [PubMed: 6854644]
39. Op den Kamp JA, Kauerz MT, van Deenen LL. Biochim Biophys Acta. 1975; 406:169–177. [PubMed: 1191645]
40. Epand RM, Bottega R. Biochim Biophys Acta. 1988; 944:144–154. [PubMed: 3179286]
41. Grasberger B, Minton AP, DeLisi C, Metzger H. Proc Natl Acad Sci U S A. 1986; 83:6258–6262. [PubMed: 3018721]
42. Senes A, Engel DE, DeGrado WF. Curr Opin Struct Biol. 2004; 14:465–479. [PubMed: 15313242]
43. Maingret F, Patel AJ, Lesage F, Lazdunski M, Honore E. J Biol Chem. 2000; 275:10128–10133. [PubMed: 10744694]
44. Perozo E, Cortes DM, Sompornpisut P, Kloda A, Martinac B. Nature. 2002; 418:942–948. [PubMed: 12198539]
45. Vasquez V, Sotomayor M, Cordero-Morales J, Schulten K, Perozo E. Science. 2008; 321:1210–1214. [PubMed: 18755978]
46. Keller SL, Bezrukov SM, Gruner SM, Tate MW, Vodyanoy I, Parsegian VA. Biophys J. 1993; 65:23–27. [PubMed: 8369434]
47. Bezrukov SM. J Membr Biol. 2000; 174:1–13. [PubMed: 10741427]

48. Curran AR, Templer RH, Booth PJ. Biochemistry. 1999; 38:9328–9336. [PubMed: 10413507]
49. Curnow P, Lorch M, Charalambous K, Booth PJ. J Mol Biol. 2004; 343:213–222. [PubMed: 15381431]
50. Hong H, Tamm LK. Proc Natl Acad Sci U S A. 2004; 101:4065–4070. [PubMed: 14990786]
51. Bowie JU. Proc Natl Acad Sci U S A. 2004; 101:3995–3996. [PubMed: 15024105]
52. Smith SO, Song D, Shekar S, Groesbeek M, Ziliox M, Aimoto S. Biochemistry. 2001; 40:6553–6558. [PubMed: 11380249]
53. MacKenzie KR, Prestegard JH, Engelman DM. Science. 1997; 276:131–133. [PubMed: 9082985]
54. Heijne G. Embo J. 1986; 5:3021–3027. [PubMed: 16453726]
55. Krepkiy D, Mihailescu M, Freites JA, Schow EV, Worcester DL, Gawrisch K, Tobias DJ, White SH, Swartz KJ. Nature. 2009; 462:473–479. [PubMed: 19940918]
56. Chamberlain AK, Lee Y, Kim S, Bowie JU. J Mol Biol. 2004; 339:471–479. [PubMed: 15136048]
57. Liang J, Adamian L, Jackups R Jr. Trends Biochem Sci. 2005; 30:355–357. [PubMed: 15935679]
58. Hong M, Su Y. Protein Sci. 2011; 20:641–655. [PubMed: 21344534]
59. Taverna DM, Goldstein RA. Proteins. 2002; 46:105–109. [PubMed: 11746707]
60. Hong H, Joh NH, Bowie JU, Tamm LK. Methods Enzymol. 2009; 455:213–236. [PubMed: 19289208]
61. Ames BN, Dubin DT. J Biol Chem. 1960; 235:769–775. [PubMed: 13793161]

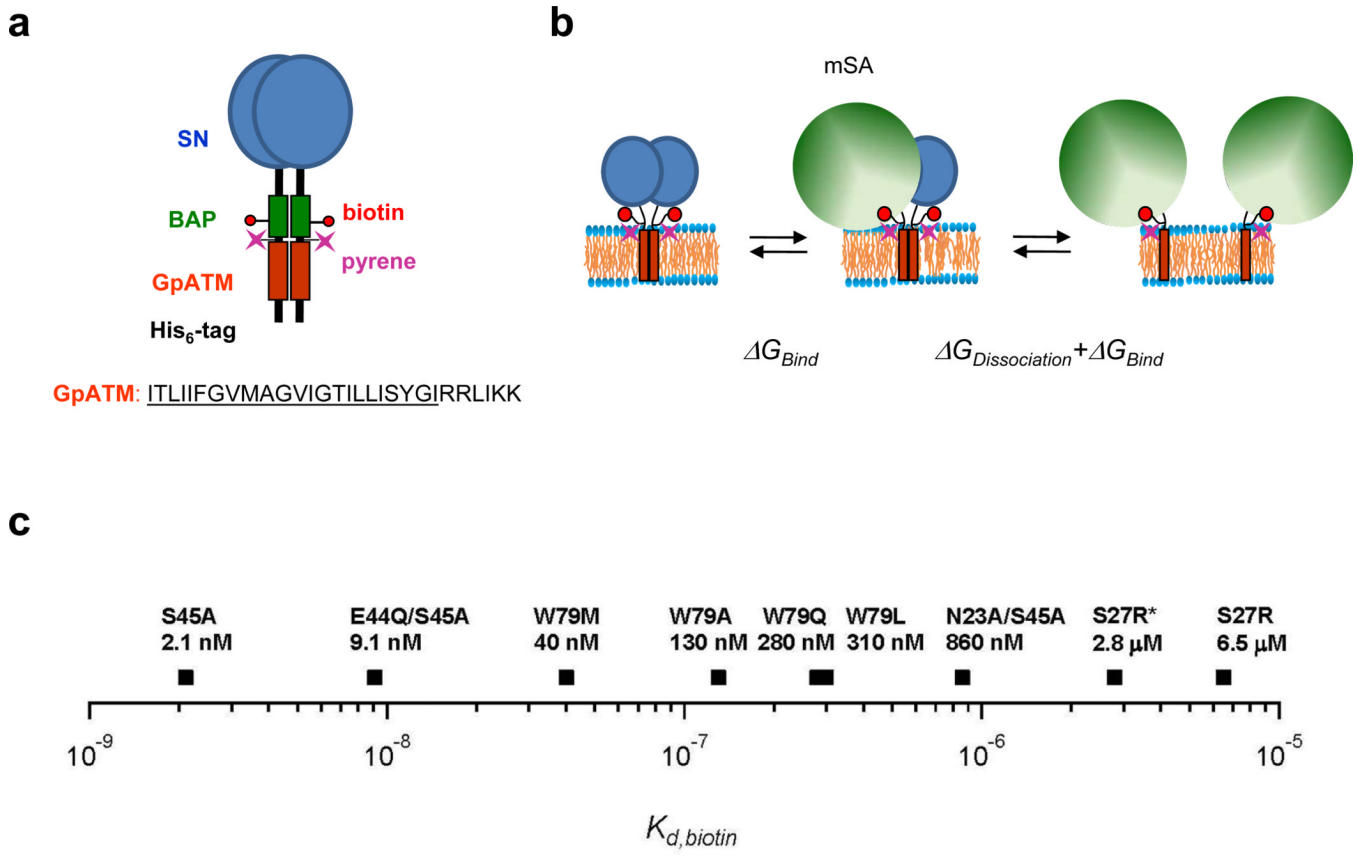

Figure 1.

The steric trap method. (a) Design of the construct used for steric trapping[24]. GpATM: orange, SN: blue (staphylococcal nuclease fused to the N-terminus), and BAP: green (biotin acceptor peptide). A unique cysteine was labeled with a pyrene fluorescent probe for the detection of binding/dissociation. The amino acid sequence of human GpATM is composed of the hydrophobic transmembrane segment (underlined) followed by a series of positively charged residues in the C-terminus. (b) Reaction scheme of the steric trap method. A single monovalent streptavidin (green sphere) can bind to one of the biotin tags in the dimer with its intrinsic binding affinity (ΔG_{bind}). Because of steric overlap in the dimeric form, however, a second streptavidin can only bind to the dissociated form. Thus, the affinity of the second streptavidin is modulated by the stability of the dimer, yielding an overall free energy of binding equal to $\Delta G_{dissociation} + \Delta G_{bind}$. (c) If the affinity of mSA is too high, binding is insensitive to the contribution from dissociation. If the affinity is too low, impractically high concentrations of mSA are required to drive dissociation. We therefore employ a library of mSA mutants with various intrinsic biotin binding affinities ($K_{d\ biotin}$)[24]. mSA-S27R (asterisk) has a stronger biotin binding affinity in the negatively charged membranes than in neutral lipid environments (see text).

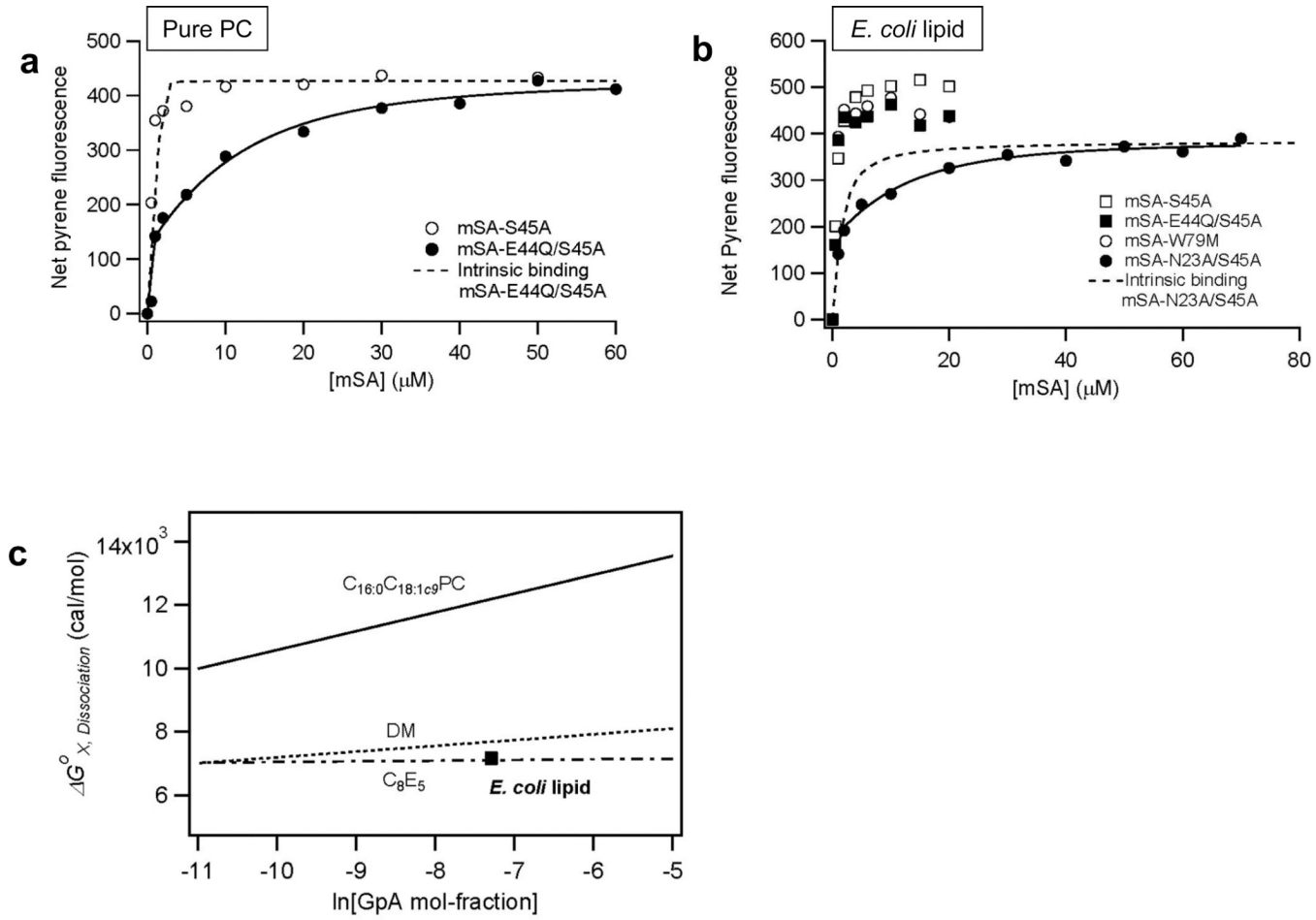

Figure 2.

Comparison of of SNGpA dimer in pure PC and *E. coli* lipid bilayers. (a) mSA binding curves in pure $C_{16:0}C_{18:1c9}$PC. The affinity of mSA-S45A is too high under these conditions to observe a second binding phase from dissociation, but the mSA-E44Q/S45A mutant ($K_{d,biotin}$=9.1×10^{-9} M) allows the dissociation phase to be observed. The fitted $K_{d,GpA}$ of GpATM dimer was 1.5±0.6×10^{-12} M at *L/P*=1000 with mSA-E44Q/S45A. (b) Selection of a mutant mSA with an optimal $K_{d,biotin}$ to extract the dissociation constant ($K_{d,GpA}$) of SNGpATM dimer in *E. coli* lipid membranes. In contrast to pure PC bilayers, the mSA-E44Q/S45A variant has too high affinity to measure dissociation in *E. coli* lipid. Instead, a much lower affinity variant was required, mSA-N23A/S45A ($K_{d,biotin}$=8.6×10^{-7} M), indicative of the weaker dimerization of SNGpATM in *E. coli* lipids. For the mSA-N23A/S45A binding curve, we obtain $K_{d,GpA}$ = 1.0±0.3×10^{-8} M at a lipid-to-protein molar ratio (*L/P*) of 1500. All measurements were performed in 20 mM MOPS (pH 7.4), 200 mM NaCl buffer solutions with mSA-accessible SNGpATM concentrations of 1.8 μM. (c) Comparison of the dissociation free energy ($\Delta G_{X,Dissociation}$) of GpATM dimer in *E. coli* lipid membranes relative to pure $C_{16:0}C_{18:1c9}$PC bilayers[24] (solid line), DM micelles[33] (dotted line), and C_8E_5 micelles[32] (dashed line). $\Delta G_{X,Dissociation}$ of GpATM dimer is expressed in mol-fraction scale[32] as a function of molar ratio of GpATM to total detergents or lipid concentrations. The lines indicating the concentration dependence of dissociation free energies in various environments were obtained previously[24,32,33].

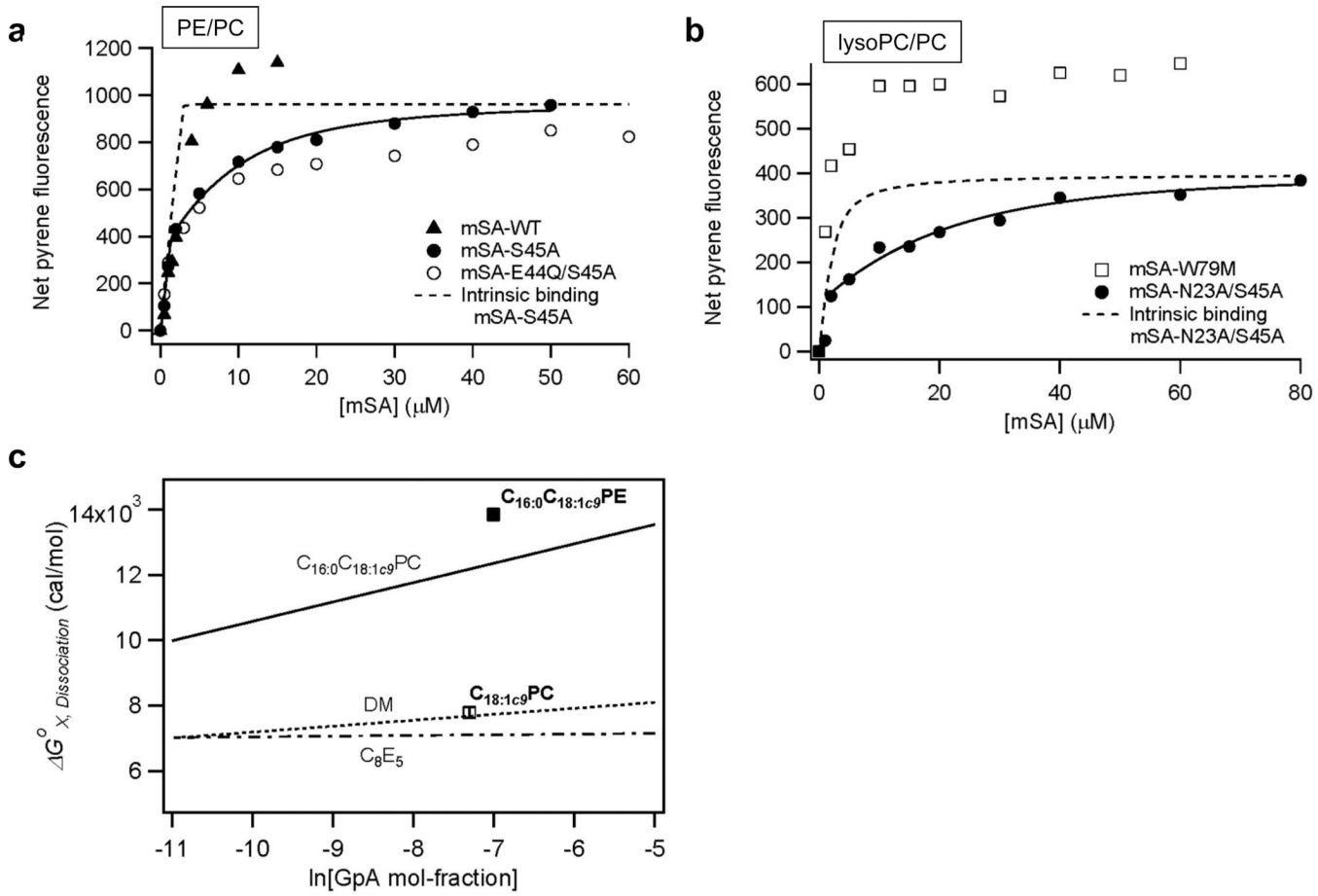

Figure 3.

Effects of bilayer lateral pressure profile on the stability of GpATM dimer. (a) mSA-binding curves in $C_{16:0}C_{18:1c9}$PE/PC (40/60) lipid bilayers. $K_{d,GpA}$=2.1±0.6×10^{-13} M was obtained at *L/P*=1100 with mSA-S45A ($K_{d,biotin}$=2.1×10^{-9} M). (b) mSA binding curves in $C_{18:1c9}$PC/$C_{16:0}C_{18:1c9}$PC (20/80) bilayers. $K_{d,GpA}$=6.0±2.4×10^{-9} M was obtained at *L/P*=1500 with mSA-N23A/S45A ($K_{d,biotin}$=8.6×10^{-7} M). (c) Summary of changes in $\Delta G_{X,Dissociation}$ induced by 40 mol-% $C_{16:0}C_{18:1c9}$PE (filled square) and 20 mol-% $C_{18:1c9}$PC (empty square) relative to pure $C_{16:0}C_{18:1c9}$PC bilayers. The lines indicating the concentration dependence of dissociation free energies in various environments were obtained previously[24,32,33].

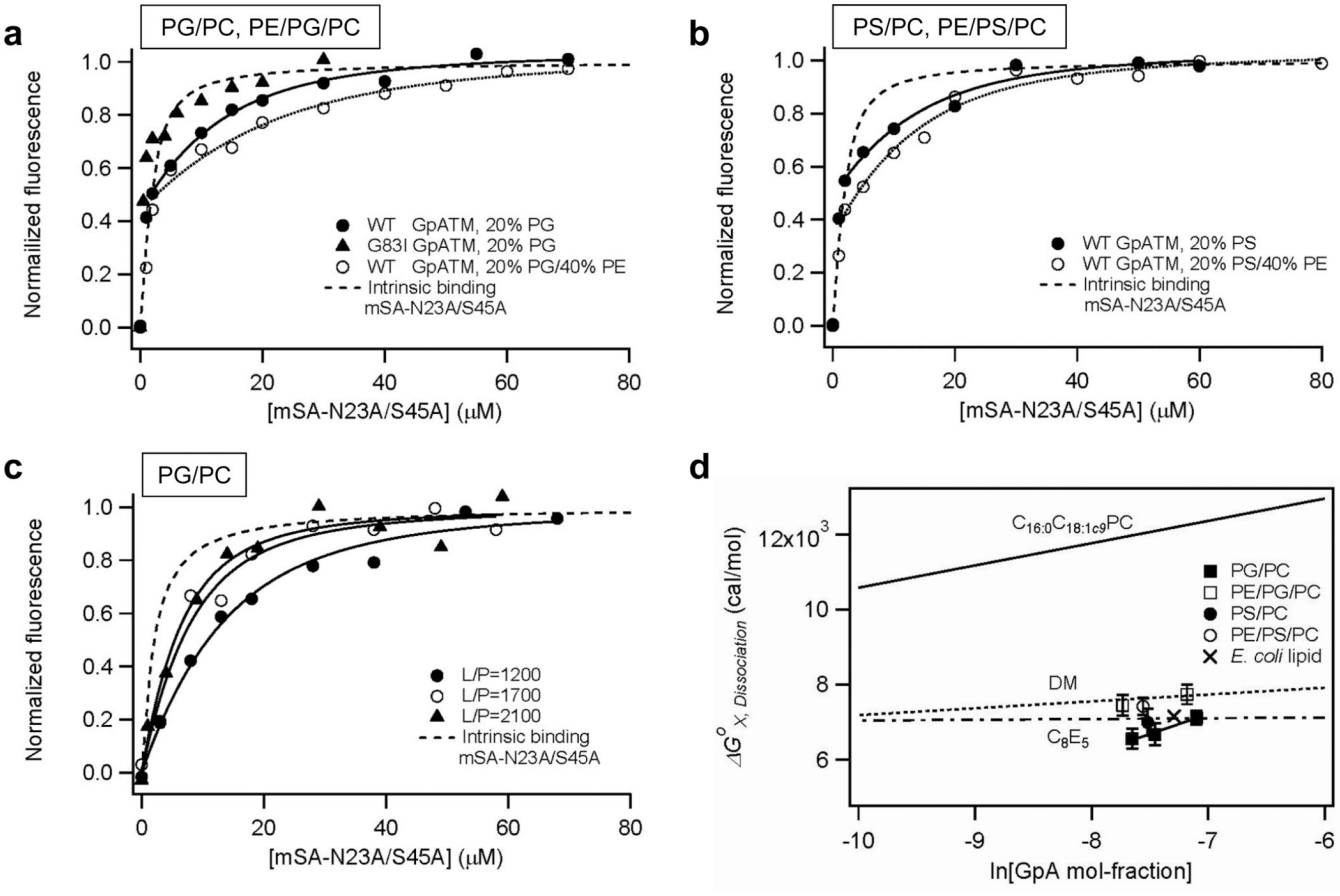

Figure 4.

The effect of negatively charged lipids on SNGpATM dimer affinity. (a) mSA binding curves of wild-type and non-dimerizing G83I GpATM mutant in $C_{16:0}C_{18:1c9}$PG/PC (20/80) and wild-type GpATM in $C_{16:0}C_{18:1c9}$PE/PG/PC (40/20/40) bilayers at *L/P*=1200~1300. $K_{d,GpA}$=1.4±0.4×10^{-8} M and $K_{d,GpA}$=5.1±2.2×10^{-9} M were obtained in $C_{16:0}C_{18:1c9}$PG/PC and $C_{16:0}C_{18:1c9}$PE/PG/PC, respectively, using a weaker biotin binding mSA-N23A/S45A ($K_{d,biotin}$=8.6×10^{-7}M). (b) mSA binding curves of wild-type GpATM in $C_{16:0}C_{18:1c9}$PS/PC (20/80) and $C_{16:0}C_{18:1c9}$PE/PS/PC (40/20/40) bilayers at *L/P*=1800~1900. $K_{d,GpA}$=2.5±1.5×10^{-8} M and $K_{d,GpA}$=1.0±0.4×10^{-8} M were obtained in $C_{16:0}C_{18:1c9}$PS/PC and $C_{16:0}C_{18:1c9}$PE/PS/PC, respectively, using mSA-N23A/S45A ($K_{d,biotin}$=8.6×10^{-7}M). (c) Dilution effects of GpATM in the negatively charged $C_{16:0}C_{18:1c9}$PG/PC (20/80) membranes. The fitted $K_{d,GpA}$'s were 1.4±0.4×10^{-8} M at *L/P*=1200, 3.2±1.6×10^{-8} M at *L/P*=1700, and 4.7±2.1×10^{-8} M at *L/P*=2100. (d) Summary of the effects of negatively charged lipids. $C_{16:0}C_{18:1c9}$PG/PC (20/80) and $C_{16:0}C_{18:1c9}$PS/PC (20/80) destabilize the SNGpATM dimer relative to pure $C_{16:0}C_{18:1c9}$PC bilayers. A modest stabilization by the introduction of $C_{16:0}C_{18:1c9}$PE can be seen by the increase of dissociation free energies in $C_{16:0}C_{18:1c9}$PE/PG/PC (40/20/40) and $C_{16:0}C_{18:1c9}$PE/PS/PC (40/20/40) bilayers. The stability of GpATM dimer in *E. coli* lipid membranes is also indicated for comparison. The lines indicating the concentration dependence of dissociation free energies in various environments were obtained previously[24,32,33].

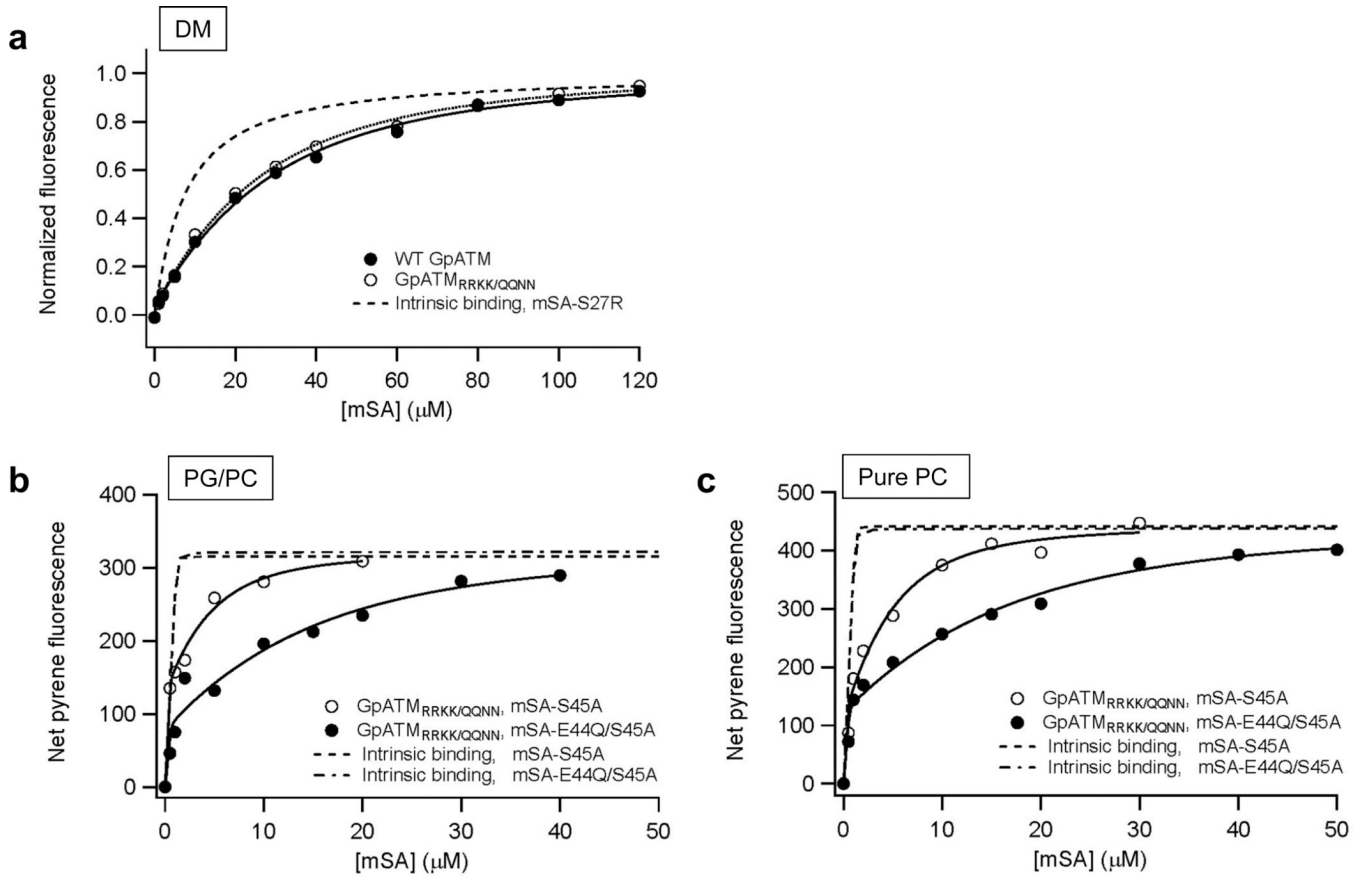

Figure 5.

Stability of the neutral GpATM$_{RRKK/QQNN}$ in various lipid environments. (a) Binding curves of mSA-S27R to 2 μM wild-type SNGpATM ($K_{d,GpA}$=1.7±0.3×10^{-7} M) and SNGpATM$_{RRKK/QQNN}$ ($K_{d,GpA}$=2.6±0.6×10^{-7} M) in 40 mM DM micelles. (b) mSA binding curves of SNGpATM$_{RRKK/QQNN}$ in the negatively charged $C_{16:0}C_{18:1c9}$PG/PC (20/80) bilayers at *L/P*=2100. The stability of the dimer was probed using mSA-S45A ($K_{d,GpA}$=4.8±2.5×10^{-13} M) and mSA-E44Q/S45A ($K_{d,GpA}$=7.3±4.1×10^{-13} M). (c) mSA binding curves of SNGpATM$_{RRKK/QQNN}$ in neutral $C_{16:0}C_{18:1c9}$PC bilayers at *L/P*=1900. The stability of the dimer was probed using mSA-S45A ($K_{d,biotin}$=2.1×10^{-9} M, $K_{d,GpA}$=4.0±2.2×10^{-13} M) and mSA-E44Q/S45A ($K_{d,biotin}$=9.1×10^{-9} M, $K_{d,GpA}$=5.8±2.4×10^{-13} M).

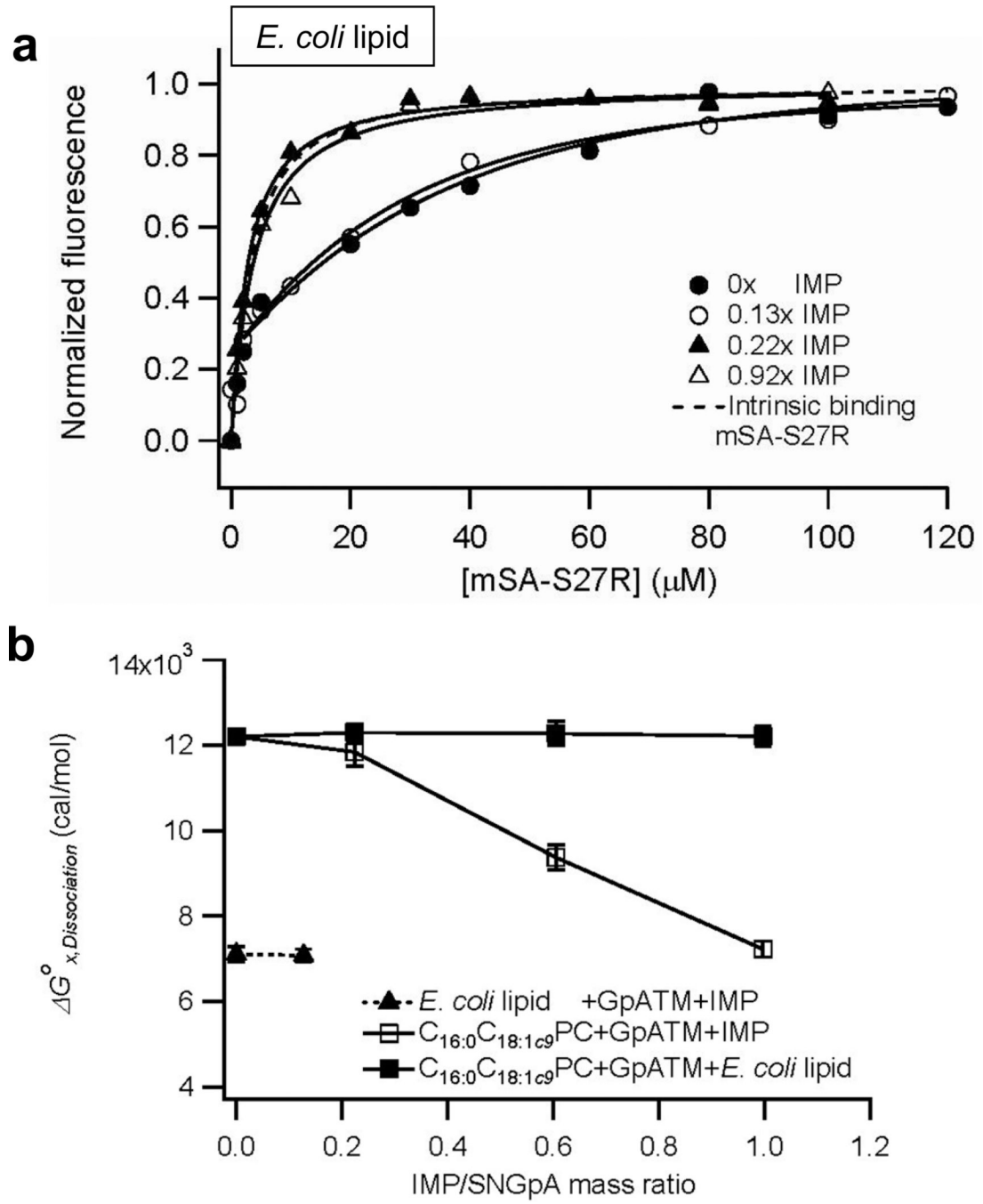

Figure 6.

Effects of total *E. coli* inner membrane protein extracts (IMP) on the stability of SNGpATM dimer. (a) Binding curves of mSA-S27R to 2.1~2.7 μM SNGpATM with an increasing amount of IMPs in *E. coli* lipid membranes at *L/P*=1500. The fitted $K_{d,GpA}$'s were $1.1\pm0.4\times10^{-8}$ M and $1.4\pm0.3\times10^{-8}$ M at the IMP to SNGpATM mass ratios of 0 and 0.13, respectively. At higher mass ratios, the dissociation constant was too weak to measure, even with our lowest affinity mSA variant. (b) Changes in the dissociation free energies ($\Delta G_{X,Dissociation}$) of the SNGpATM dimer as a function of the mass ratio of IMPs to SNGpATM in *E. coli* lipid and $C_{16:0}C_{18:1c9}$PC membranes. For the detailed experimental design and data, see the Supporting Figure 7.

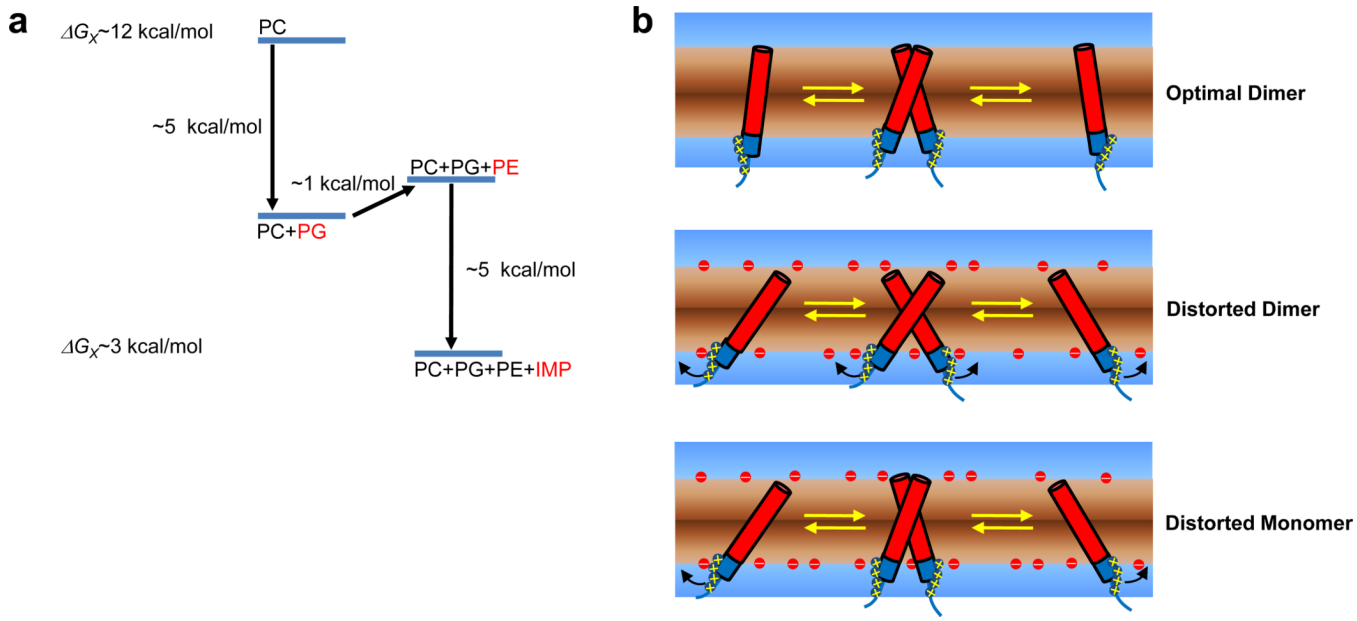

Figure 7.

Summary of the effects of membrane components on GpATM dimer stability. (a) Major environmental forces which contribute to the weak TM helix-helix interactions in natural cell membranes. Relative to neutral fluid $C_{16:0}C_{18:1c9}$PC bilayers, the negatively charged lipids such as PG and PS dominate the lipid effects, destabilizing the dimer by ~5 kcal/mol. The increased elastic stiffness by the inverted hexagonal phase forming PE lipids mildly stabilizes the dimer. The addition of non-specific proteins to the membranes can further destabilize the specific helix-helix interactions. (b) Possible models for the destabilization of GpATM in the negatively charged membranes. In neutral membrane vesicles, the dimer is stabilized by the restricted lateral and angular motions (top). In the negatively charged membranes, however, interfacial positively charged Arg and Lys residues of TM helices are strongly attracted to the negatively charged lipid headgroups. The resulting adjustment of each monomeric TM helix relative to bilayer normal may cause the distortion of the dimer interface from the optimal side-chain packing destabilizing the dimer (middle). It is also possible that the optimal dimer packing is maintained, but the significant free energy cost is required to form a dimer from a structurally altered, electrostatistically stabilized monomer.